



Delft University of Technology

Innovative floating bifacial photovoltaic solutions for inland water areas

Ziar, Hesan; Prudon, Bjorn; Lin, Fen Yu; Stark, Tim; Teurlincx, Sven; Goma, Elias Garcia; Alavez, Ignacio Narvaez; Santbergen, Rudi; Isabella, Olindo; More Authors

DOI

[10.1002/pip.3367](https://doi.org/10.1002/pip.3367)

Publication date

2020

Document Version

Final published version

Published in

Progress in Photovoltaics: research and applications

Citation (APA)

Ziar, H., Prudon, B., Lin, F. Y., Stark, T., Teurlincx, S., Goma, E. G., Alavez, I. N., Santbergen, R., Isabella, O., & More Authors (2020). Innovative floating bifacial photovoltaic solutions for inland water areas. *Progress in Photovoltaics: research and applications*, 29 (2021)(7), 725-743. <https://doi.org/10.1002/pip.3367>

Important note

To cite this publication, please use the final published version (if applicable).
Please check the document version above.



Copyright

Other than for strictly personal use, it is not permitted to download, forward or distribute the text or part of it, without the consent of the author(s) and/or copyright holder(s), unless the work is under an open content license such as Creative Commons.

Takedown policy

Please contact us and provide details if you believe this document breaches copyrights.
We will remove access to the work immediately and investigate your claim.

Innovative floating bifacial photovoltaic solutions for inland water areas

Hesan Ziar¹  | Bjorn Prudon² | Fen-Yu (Vicky) Lin³ | Bart Roeffen³ |
 Dennis Heijkoop⁴ | Tim Stark¹ | Sven Teurlincx⁵ | Lisette de Senerpont Domis^{5,6} |
 Elias Garcia Goma¹ | Julen Garro Extebarria¹ | Ignacio Narvaez Alavez¹ |
 Daniel van Tilborg⁴ | Hein van Laar⁴ | Rudi Santbergen¹ | Olindo Isabella¹ 

¹Photovoltaic Materials and Devices Group, Delft University of Technology, Mekelweg 4, Delft, 2628 CD, The Netherlands

²Waterschap Rivierenland, De Blomboogerd 1, Tiel, 4003 BX, The Netherlands

³Blue21 B.V., Molengraaffsingel 12, Delft, 2629 JD, The Netherlands

⁴Hakkers B.V., Oudsas 11, Werkendam, 4251 AW, The Netherlands

⁵Department of Aquatic Ecology, Netherlands Institute of Ecology (NIOO-KNAW), Droevendaalsesteeg 10, Wageningen, 6708 PB, The Netherlands

⁶Aquatic Ecology and Water Quality Management Group, Wageningen University & Research, Wageningen, The Netherlands

Correspondence

Hesan Ziar, Photovoltaic Materials and Devices Group, Delft University of Technology, Mekelweg 4, 2628CD Delft, The Netherlands.
 Email: h.ziar@tudelft.nl

Abstract

Photovoltaic (PV) technology has the potential to be integrated on many surfaces in various environments, even on water. Modeling, design, and realization of a floating PV system have more challenges than conventional rooftop or freestanding PV system. In this work, we introduce two innovative concepts for floating bifacial PV systems, describing their modeling, design, and performance monitoring. The developed concepts are retractable and enable maximum energy production through tracking the Sun. Various floating PV systems (monofacial, bifacial with and without reflectors) with different tilts and tracking capabilities are installed on a Dutch pond and are being monitored. Results of the thermal study showed that partially soaking the frame of PV modules into water does not bring a considerable additional yield (+0.17%) and revealed that floating PV modules experience higher temperature special variance compared with land-based systems. Observations showed that the birds' presence has a severe effect on floating PV performance in the short term. Electrical yield investigation concluded that due to low albedo of inland water areas (~6.5%), bifacial PV systems must have reflectors. One-year monitoring showed that a bifacial PV system with reflector and horizontal tracking delivers ~17.3% more specific yield (up to 29% in a clear-sky month) compared with a monofacial PV system installed on land. Ecological monitoring showed no discernable impacts on the water quality in weekly samplings but did show significant impacts on the aquatic plant biomass and periods of low oxygen concentrations.

KEYWORDS

bifacial PV, ecology, floating PV (FPV), island, modeling, monitoring, onshore, partial water soaking, photovoltaic (PV) module, PV system, realization, retractable, tracker

1 | INTRODUCTION

Bifacial photovoltaic (PV) technology (cells and modules) can absorb light simultaneously from the front and rear sides.¹ This feature

brings important advantages concerning monofacial PV technology: (1) lower land-use for the same watt-peak installation, (2) lower levelized cost of electricity (LCOE), and (3) smoother daily power profile. Having such advantages and lowering the manufacturing

This is an open access article under the terms of the Creative Commons Attribution License, which permits use, distribution and reproduction in any medium, provided the original work is properly cited.

© 2020 The Authors. Progress in Photovoltaics: Research and Applications published by John Wiley & Sons Ltd

cost have increased the bifacial PV installation rapidly from 97 MWp in 2016 to over 5 GWp in 2019.² The market share of bifacial technology is expected to grow from ~15% in 2019 to ~70% by 2030.³

On the other hand, the expected increasing trend for the world population,⁴ and subsequently the need for food and energy, signifies the importance of the land. In such a situation, floating PV (FPV) systems either on off-shore or on-shore water areas seems like an interesting option to reduce the LCOE and the conflict with other land-user sectors such as agriculture and housing. Installation of PV systems on ocean water brings several challenges such as harsh dynamics, storms, and difficult accessibility. Inland water areas could be instead exploited for clean solar energy production in several countries, such as Germany, Finland, and the Netherlands. For the case of the Netherlands, 17% of the land is covered by waterways, lakes, and ponds.⁵ Moreover, in countries with high insolation rate and drinkable water scarcity, FPV can produce electricity and prevent water evaporation as well.⁶ For example, in Morocco, 3 m³ of water is evaporated yearly per each square meter of water surface behind the dams.⁷ The market share of the FPV system is expected to be >10% by 2030.³

Combining these two trends in the PV industry, floating and bifacial, could be a promising way forward. However, floating bifacial PV has rather unique requirements, challenges, and opportunities. There is general understanding in the literature that FPV systems face wave and wind forces with various frequency and domains,⁸ experience stronger aging mechanisms caused by moisture and harsh environment^{9,10} while they might benefit from the cooler working environment and sunlight reflection from the water.¹¹ They should also meet the requirement for water ecology, release minimum or zero toxic material to the water, and enable mowing activities. Moreover, as with any novel technology, bifacial and FPV is still held back by a lack or inaccessibility of long-term field data to demonstrate its real-world performance under various conditions.¹² Therefore, provided that the requirements are met and challenges were overcome, combining bifacial PV and floating systems can bring additional energy yield and keep the land usage rate low.

The aim of this work is to model, design, and monitor floating bifacial PV systems for inland water areas. To realize these research goals, the INNOvative ZOn-pv op Water (INNOZOWA) consortium was formed in 2017 by Delft University of Technology, Waterschap Rivierenland,¹³ Hakkers BV,¹⁴ and Blue21 BV.¹⁵ Main steps were

(1) location survey and accurate PV yield modeling, (2) innovative, applicable, and modular design and realization of the floating construction and PV systems, and (3) monitoring for the systems. These three main steps are discussed in detail in Sections 2 to 4 of this paper. In chapter 5, key messages of this research are highlighted. Throughout the study, several interesting facts about floating bifacial PV were proven and/or observed that some are in contrast with initial expectation.

2 | LOCATION SURVEY AND MODELING

2.1 | Location

A storm water pond, located in Weurt, Eastern Netherlands, was selected for this research (see Figure 1). Based on the measurement, the basin has a minimum depth of 0.9 m and up to 1.9 m in the deeper parts. Depending on the season and water retention plans, the basin can occupy an area of 18 524 to 22 639 m.²

2.2 | Horizon and sky view factor

Skyline-related information is an important input for PV yield modeling that influences the direct and diffuse components of the sunlight.¹⁶ One key indicator is sky view factor (SVF), which is a unit-less quantity that represents the ratio between the visible sky and a hemisphere centered over the studied location.^{17,18} Skyline information is extracted using a hori-catcher (see Figure 2A)¹⁹ in and around the pond at several spots with different heights. Then, the captured horizon was processed using Meteororm software package²⁰ using the approach described in Stein²¹ and Keijzer.²² Further, by applying linear interpolation, a map of SVF was obtained, as can be seen in Figure 2B.

2.3 | Albedo

Albedo is measured by dividing the incoming global radiant fluxes reaching on the down-facing and up-facing parts of a surface. Location, time, geometry, and weather conditions influence the value of albedo.²³ Albedo is spectrally dependent, and for PV applications, the



FIGURE 1 Panoramic view of the artificial pond located in Weurt, the Netherlands (51.8514°N, 5.7950°E). The pond is developed as a water retention basin. The pond has a rectangular shape, not perfectly aligned with the south. The longer side of the pond is 42° deviated toward the west (222°) [Colour figure can be viewed at wileyonlinelibrary.com]

FIGURE 2 (A) A hori-catcher image at one spot in the pond taken using an upside-down camera and a mirror-like spherical cap. (B) Interpolated map of the sky view factor (%) for the pond area. The sky view factor (SVF) changes between 97.9% and 99.3%, showing an almost free horizon suitable for PV installation. One meter above the water surface was considered for SVF calculation as SVF does not significantly depend on few meters of change in the altitude [Colour figure can be viewed at wileyonlinelibrary.com]

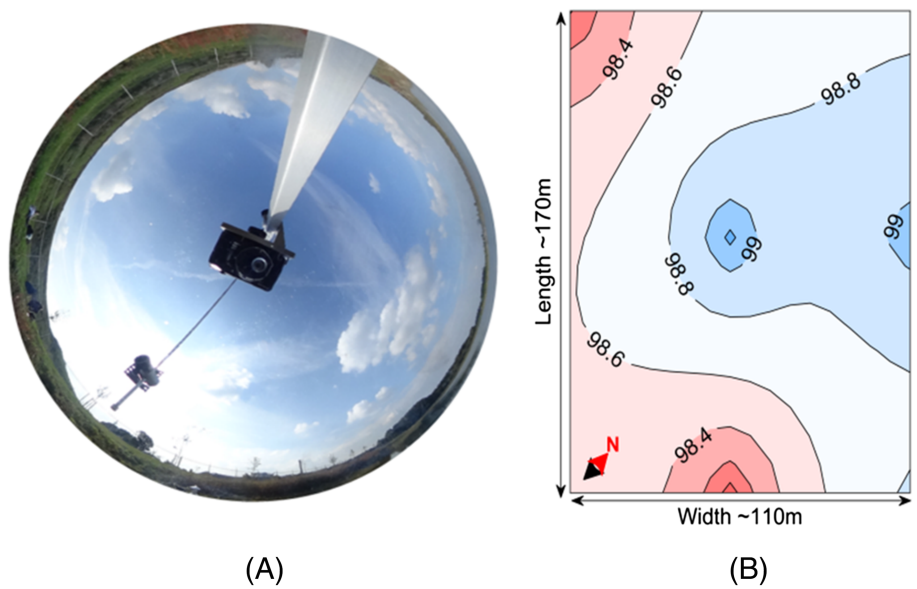


FIGURE 3 (A) Broadband (285–2,800 nm), and (B) spectrally resolved (278–1098 nm) albedo measurements at two different spots in the pond [Colour figure can be viewed at wileyonlinelibrary.com]



effective albedo, which considers the spectral response of the PV cell, should be taken into account.²⁴ Accurate assessment of albedo becomes more important for bifacial PV installations. Broadband and spectrally resolved albedos were measured both for the water in and the soil around the pond. Figure 3 shows the Kipp&Zonen albedometer (sensitive from 285 to 2800 nm, measures in W/m^2) and Avantes spectrometer (sensitive from 278 to 1098 nm, measures in $\mu W/cm^2/nm$), which were used, respectively, to measure the broadband and spectrally resolved albedos at various spots at the pond. Then, by applying the model described in ZiAR et al.,²³ which bounds the geometrical and spectral features of albedo, maximum value of albedo was calculated for various levels above the water surface at the pond. The mapped albedos of the pond at 1 and 2 m above water level are shown in Figure 4. As it can be seen, the closer to the shore and the higher from the water surface, the higher the albedo. Figure 5A shows the spectrally resolved reflected irradiance of the soil and the water at the pond, whereas Figure 5B shows two sky spectra: measured at the site and standard ASTM G173. Figure 5C shows the typical response of a monocrystalline silicon solar cell.²⁵ Using the information given in Figure 5, the effective albedo of the soil and water are calculated as follows: 15.64% (soil), 7.71% (water 0.5 m depth), and 8.11%

(water 1 m depth). Very low albedo of water predicts a low contribution of the reflected light energy for bifacial PV installation and, therefore, suggests the necessity for using reflectors.

2.4 | Yearly irradiation modeling

Monofacial PV brings the advantage of simplicity and lower costs, whereas bifacial FPV are expected to yield more.^{26,27} Therefore, in our preinstallation study, we considered both monofacial and bifacial technologies. Monofacial PV modules can be either placed aligned with the pond orientation for better area usage (higher kWh/m^2) or toward the south for better performance (higher kWh/kWp). For bifacial PV, reflector type and orientation and its distance from the PV module are also becoming important.

During the preinstallation study, several design parameters (type and technology of the PV modules, BoS components, etc.) had not been fixed; therefore, the focus was put on the irradiation modeling. Since irradiation is the key component in PV yield analysis²⁸ the design that receives the highest yearly irradiation will yield higher electrical output.

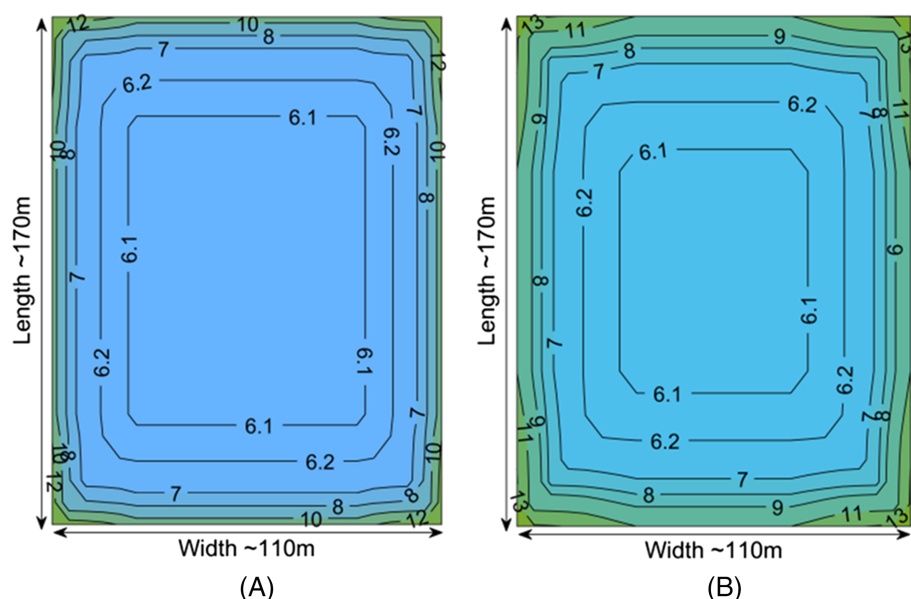


FIGURE 4 Mapped broadband albedo (%) for the pond area at (A) 1 m above water level and (B) 2 m above water level [Colour figure can be viewed at wileyonlinelibrary.com]

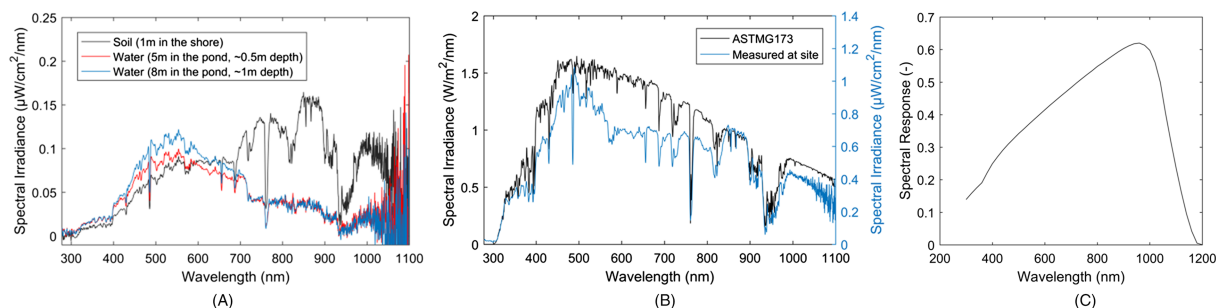


FIGURE 5 Spectrally dependent data for effective albedo calculations. (A) Reflected spectrum measured at the pond for the soil and two different depth of water. (B) Measured sky spectral irradiance and the ASTM G173 standard global irradiance.²⁹ (C) Spectral response of HOQ mono-cSi reference cell reported by Fraunhofer ISE.²⁵ Measurements were done on November 29, 2017, under overcast sky condition, no rain, ambient temperature 2°C, and the wind speed of 0.5 to 1 m/s. Effective albedo values for the soil, 5 m, and 8 m in the pond are, respectively, calculated as 15.64%, 7.71%, and 8.11%. Considering ASTM G173 sky spectrum will change the values slightly (15.34%, 7.91%, and 8.32%). It is worth noting that for assessing the effective albedo, when the target PV technology is known, relative response of that technology should be used. Note that the front side and rear side responses of bifacial PV modules are different³⁰ [Colour figure can be viewed at wileyonlinelibrary.com]

Using the location inputs described in Sections 2.1–2.3, several preinstallation yield simulations were done, and the result is presented in this section.

The pond is located between five meteorological stations of the KNMI (Koninklijk Nederlands Meteorologisch Instituut) network³¹ (see Figure 6). By retrieving the 1-h resolution global horizontal irradiance (GHI) data from the stations and applying inverse distance weighted (IDW) method,³² the GHI data at Weurt was interpolated and then processed in Meteonorm (horizon was applied) and further broken into direct normal and diffuse horizontal irradiances (DNI and DHI) through BRL decomposition model,³³ which was shown to be the most accurate irradiation decomposition model for the morphology of the Netherlands.³⁴ The location receives the irradiation of ~989 kWh/m²/year. Table 1 shows the calculated yearly irradiation for various fixed and tracking monofacial PV modules. The simulated tracking system was astronomically tracking the Sun position.

Further, to assess the total yearly irradiation on bifacial PV modules, the PVMD toolbox was used.³⁶ Several cases were studied with various tilt and orientation for the PV module and the reflector, from which a few examples are shown in Figure 7. Simulations showed that putting a reflector very close to the bifacial PV module and relying on the light passing through the cells will not significantly contribute to the total irradiation and should be placed with a distance underneath the bifacial PV module.

The only monofacial option (see Table 1) that can outperform the tilted bifacial with a horizontal reflector (Figure 7F) is when a free-angle dual-axis tracking is done. However, this may not be mechanically feasible that tumbling a floating system might escalate the wind force. Therefore, tracking should be done within a limited range of safe angles. This suggests that maybe a tracking bifacial PV system with limited angles can bring both safe operation, long life-time, high yield, and consequently low LCOE. Therefore, in the design phase, we

a possibility in this research, we investigated a partial frame soaking of the PV module.

COMSOL Multiphysics was used to make a comparison between a bifacial PV module placed above the water and a module with direct water contact of the lower frame (see Figure 8). Water temperature, as an input for the COMSOL model, was calculated using the empirical model suggested in Harvey et al.,³⁹ whereas the rest of the weather inputs were obtained as described in Section 2.4. Material properties of the PV module layers were obtained from the literature³⁸ and are shown in Table 2. Figure 8 shows a comparison for the two simulation cases for May 30 at 13:30 at the pond location. The temperature at the bottom part of the module is considerably lower for the case where the module is placed in contact with water, but this effect is hardly extended further to the PV cells placed at the bottom. This is due to the low thermal conductivity of both the EVA and the glass. Similar COMSOL simulations were done for the daylight hours of the hottest days of the months (data of the year 2005), and further, the differences in the electrical yield were calculated. Figure 9 shows the difference between the water and the air temperatures at the pond and the additional energy gain by lower frame soaking of the bifacial PV module. The total yearly gain is very minor, around 0.17%. Considering the low energy gain and the higher chance for the potential induced degradation (PID) effect,⁴⁰ this option is left outside the perspective of a durable floating bifacial PV system.

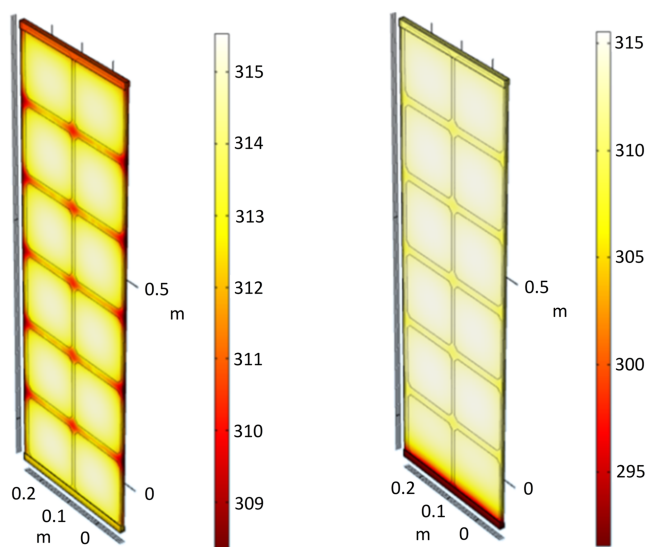


FIGURE 8 Temperature distribution (in kelvin) within the bifacial PV module without contact with water (left) and with the bottom frame in contact with water (right). The two cases are simulated using the weather data of May 30 at 13:30 at Weurt, the Netherlands. To reduce the computation burden, the simulated module was assumed to have 2×6 cells. 60-cell LG Neon 2Bifacial datasheet was used for the cell, spacing, and frame sizes. Properties of materials such as EVA and the glass were added manually using the data shown in Table 2, reported in.³⁸ For the simulations, weather data of the year 2005 was used [Colour figure can be viewed at wileyonlinelibrary.com]

3 | DESIGN AND REALIZATION

3.1 | Previous FPV concepts

After the first FPV system built in 2007 in Aichi, Japan, several FPV concepts were developed.⁴¹ A FPV system normally consists of floats, mooring, and anchoring system, PV modules, and balance of system (BoS) components. The most common float types are (1) *pure floats* with high-density polyethylene material and (2) *pontoons* (or hollow cubes) with metal trusses.^{41–43} The first type is lightweight and thin with large water-plastic contact area (at least 50% of the plant size), which increases the chance for plastic defoliation. The lightness of the floats makes it vulnerable to high wind loads^{44,45} when wave force is present, increasing the chance for the wind to blow under the floats and push them upward in a cascaded manner. The first type has a complex mooring system, hardly customizable for sun tracking and bifacial PV installation, and for a large surface, it is not sufficient to anchor the system only on the perimeter. However, it is a cost effective solution that enables large scale deployment. For example, the Hydrelia® floats developed by Ciel et Terre⁴⁶ is used in the largest Europe FPV system (17 MW) in France.⁴⁷ The second type suffers from high cost and complex construction⁴⁸ but brings the possibility for vertical sun tracking, bifacial PV, and higher tilt installation. A good example is the ~450 kW FPV installation in Swiss Alps.⁴⁹

Several concepts are introduced in the literature and patented to implement sun tracking to the floats.^{50–52} They can be categorized as trackers with and without confining structure. Almost all the FPV tracking solutions reported in the literature turns the floaters (vertical-axis sun tracking) and do not tumble them (horizontal-axis sun tracking), driven mainly by safety reasons (tumbling increases the wind load). However, turning an array of the PV modules (changing the azimuth) while their tilt is kept low because of the wind safety measures does not in principle contribute much in electric yield increase. Note that there are approaches that tilt the PV modules (not the floating structure) for horizontal sun tracking⁵³ while keeping the floating platform fixed or even rotating it to enable dual axis sun tracking.⁵⁴

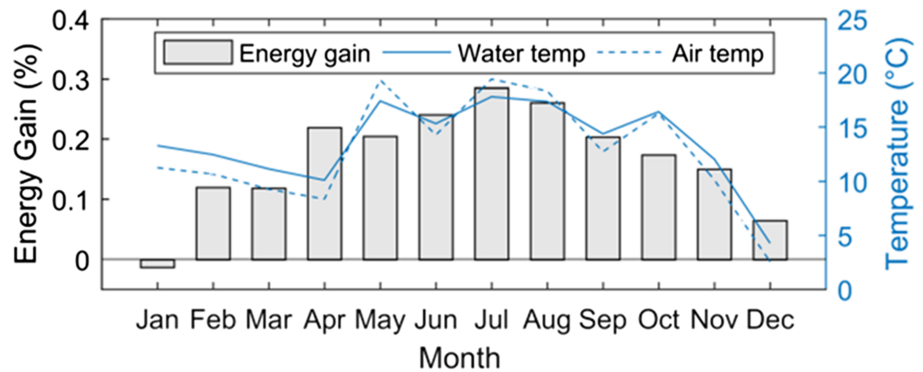
From wave point of view, there are four categories for the FPV systems. The first three categories are for inland water areas, respectively, for negligible, 1-m-, and 2-m-wave heights. The fourth category is for the open seas for which the FPV systems should withstand waves up to 10 m of height.⁵⁵ Comparative projects running at various places in the world, such as in Oostvoornse-Meer in the Netherlands,⁵⁶ show that the technology readiness level is higher for the lower wave categories; however, there is still limited practical knowledge about the long-term performance and longevity.

Further, accessibility to water areas is crucial for inland water ponds, canals, and rivers. For example, mowing activities are regularly done on inland water areas, and therefore, a sophisticated FPV system must be movable while sustaining the maximum possible electrical yield (to have a low LCOE) while being resilient to high wind and categorized wave forces.

TABLE 2 Properties of the main materials within the PV module, used in COMSOL simulation

Material	Thermal conductivity κ (W/m K)	Density ρ (kg/m ³)	Heat capacity C_p (J/kg K)	Emissivity ϵ
Silicon	130	2329	700	-
Aluminum	238	2700	900	0.77
EVA	0.34	935	480	-
Glass	1.8	2700	750	0.84
Silver	429	10 500	235	-

FIGURE 9 Air temperature, water temperature, and energy gain comparison of a frame-soaked floating bifacial PV module with a case with no direct contact with water. Hottest day of each month (year 2005) was simulated in COMSOL as the monthly representative of the PV module thermal performance. Further the electrical yield was calculated using the temperature coefficients of the 60-cell LG Neon 2Bifacial PV module [Colour figure can be viewed at wileyonlinelibrary.com]



3.2 | Introduced FPV concepts

The available knowledge in the literature, the findings reported in Section 2, mechanical restrictions, and the requirements for water mowing activities served as inputs to converge into two new FPV concepts: (i) retractable system, and (ii) tumbler floating island. In the design concept (i) PV modules are placed between four fixed pillars (as anchoring spots) and can be lined up and spread out (using two winches) when needed. This concept resembles shopping carts where the PV panels can be folded one against the other on a similar way as the shopping carts do in a supermarket. In the design concept (ii), however, the modules are installed on a floating island that is anchored at one spot to the bottom of the lake. The island is occupied with two tanks underneath to track the sun (in the horizontal axis) by pumping water from one tank to another. Both design options enable regular mowing activities and access to the water surface. Both concepts are able to cope with water level variation even in extremely low-water-level seasons. The designed concepts are shown in Figure 10.

3.3 | Realization

In summer 2019, realization of the introduced FPV concepts was accomplished. Figure 11A–E shows a few snapshots of the realization procedure. In order to monitor the performance of the FPV concepts and compare it with conventional PV systems, two land-based PV systems were also installed by the pond. In total, nine pilot systems with different features were installed, as can be seen in Figure 12.

3.4 | Components and sensors

Installed monofacial and bifacial PV modules were respectively 60-cell LG Neon 2Black (LG330N1K-V5) and 72-cell LG Neon 2Bifacial (LG400N2T-A5). Each module is equipped with a SolarEdge P5050 power optimizer, and all are connected to a SolarEdge SE17K three-phase inverter. This arrangement made it possible to monitor the DC yield of the PV modules and reduce the effect of BoS components in the comparative study of the pilot systems.

Due to a lack of immediate supply for the desired white color reflector, orange color reflector with aluminum reflecting coating was utilized. Further, a series of indoor reflectance tests were done on the reflector sample using LAMBDA 950 spectrophotometer. The effective albedo for the reflector was calculated as 68.5% (see Figure 13), which shows that the orange reflector has a comparable albedo with respect to a weathered white reflector.

The winch system is powered up by two PV + battery units located at the two ends of the retractable system (see Figure 14). In this way, the power from the pilot system is not being used for retracting maneuver. However, the power needed for tumbling the floating island is driven from the grid, and to account for this, the pump energy consumption was calculated. The tumbling system uses four pumps to distribute water between two tanks on the two sides of the floater (each tank has two compartments). Each compartment has 1.3 m³ of space. The tracking is based on the position of the sun and is done every 15 min with the resolution of 2° using a predefined look-up table. According to the tracking lookup table, on average, it takes ~30 min to fully pump the water from one compartment to another (tumble the island for 27°). This requires 2.6 m³/h of flow rate, 45 W of input power, and according to the pump performance curve will lead to

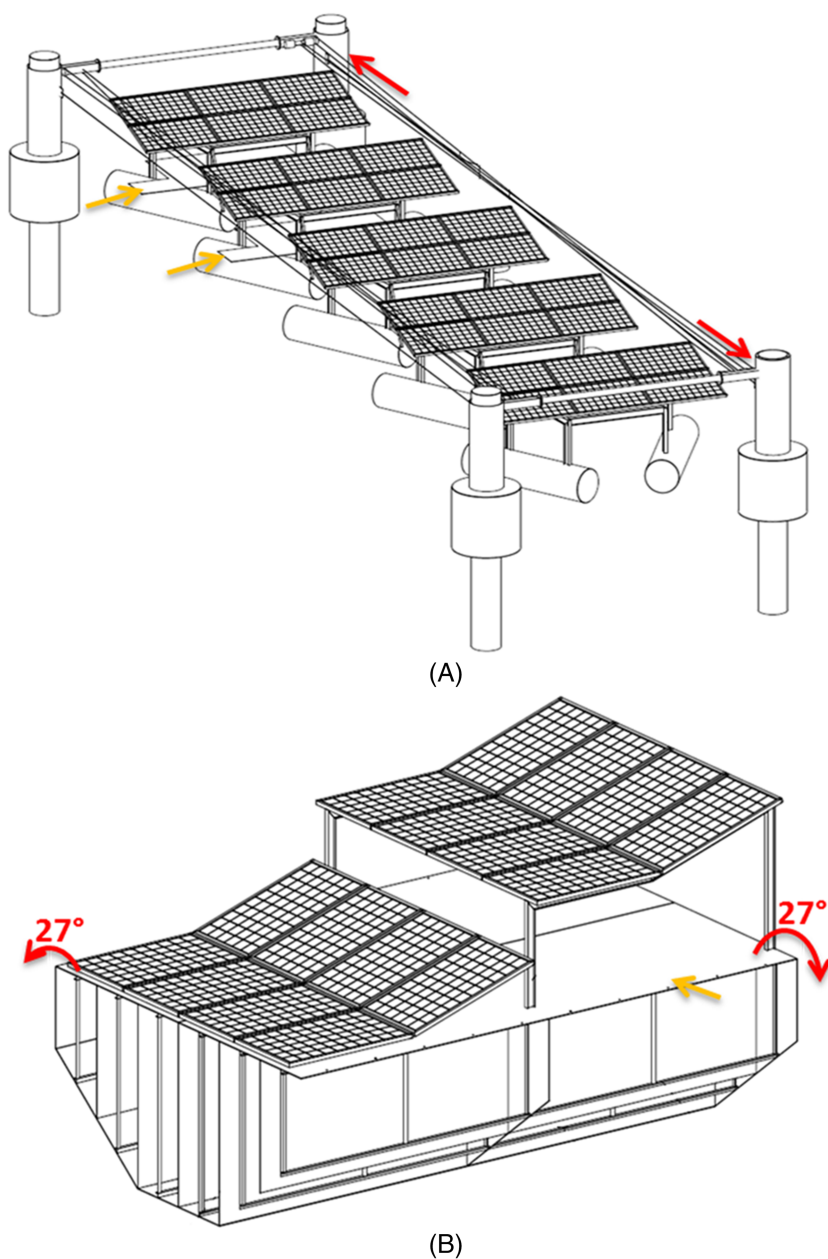


FIGURE 10 The developed floating photovoltaic (PV) concepts: (A) retractable system and (B) tumbler floating island. The retractable system has five rows of PV panels ($4.94 \text{ m} \times 2.29 \text{ m}$, 15° tilt) each with six PV modules. The distance between the panels are 4.85 m . Panels can be lined up at either two ends of the system. Reflectors (aluminum reflecting coating) can be placed under any row of the system (shown by orange arrows). The height of the PV panel upper edge from the reflector (trapezoidal shape with bases of 2.02 and 4.55 m and height of 2.01) and the water levels are 1.58 and 1.94 m . The system has the overall dimension of $25.42 \text{ m} \times 7.78 \text{ m}$. The tumbler floating island has four panels ($4.52 \text{ m} \times 1.04 \text{ m}$) of PV modules. Two rows are horizontal, and the other two are tilted for 15° . The lower and upper sides of the last row are positioned 1.33 and 1.05 m above the island surface, respectively, which is covered by aluminum reflecting coating. The island can tumble (lean to its sides) for maximum 27° to the sides and has the overall dimension of $6.62 \text{ m} \times 4.51 \text{ m}$. Red arrows show the movement capability of the designed concepts [Colour figure can be viewed at wileyonlinelibrary.com]

2.75 m of the pump head. Thus, on average every 24 h of tumbling for sun tracking consumes 90 Wh resulting in 32.85 kWh per year.

Various sensors were installed at the site at different times of the monitoring period, including a visual camera, a horizontal irradiance sensor, a wind speed sensor, an air temperature sensor, an irradiance sensor to measure the reflected sunlight by the water, and an irradiance sensor to measure the reflected light on the rear side of one bifacial PV panel with reflector. This sensor was placed on the retractable system. The sensors are shown in Figure 15.

4 | MONITORING AND ANALYSIS

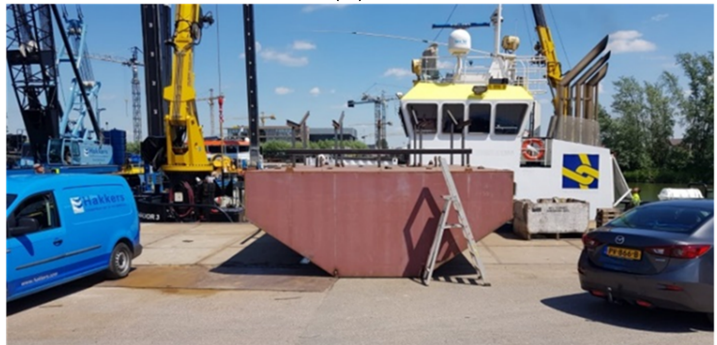
It has been reported in the literature through monitoring and simulation that the fixed FPV systems can yield $11\text{--}13\%$ more in comparison

with land-based PV systems mainly because of lower air temperature above the water and higher wind speed.^{57,58} However, expect for Liu et al.⁵⁹ that compared FPV systems with a nearby rooftop PV (probably installed at different heights thus experiencing different wind profiles) and reported $1\text{--}3^\circ\text{C}$ air temperature difference, these studies do not show a fair comparison as the PV systems do not experience the same weather condition. In Choi,⁶⁰ the two monitored PV systems were apart for 60 km , and in Golroodbari and van Sark,⁸ the implied distance between the hypothetical simulated PV systems is more than 150 km . In this research, however, we placed the land-based and the FPV systems close to each other ($\sim 50 \text{ m}$), which enables a fair comparison and a precise understanding of the long-term performance of the FPV system. Moreover, a thorough performance analysis of the floating bifacial PV systems is barely reported in the literature so far, mainly because of the complexity in both modeling and monitoring.

FIGURE 11 Snapshots of the realization procedure: (A) preparation of the floating pontoons and the attached metallic structures for the retractable systems, (B) preparation of the metallic frame for the tumbler floating island, (C) moving the retractable photovoltaic (PV) systems toward the installation spot in the pond, (D) retracting and tumbling tests on the floating concepts, and (E) operational retractable PV systems (front) and the floating island (rear) [Colour figure can be viewed at wileyonlinelibrary.com]



(A)



(B)



(C)



(D)



(E)

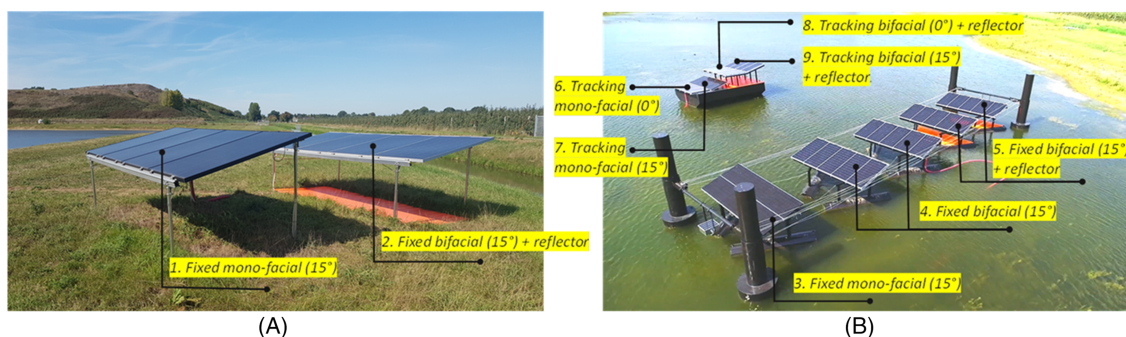


FIGURE 12 Pilot systems installed at the pond: (A) reference ground based systems by the pond and (B) installed floating photovoltaic (PV) systems. There are nine systems: (1) fixed ground based monofacial PV system, (2) fixed ground based bifacial PV system with reflector, (3) fixed floating monofacial PV system, (4) fixed floating bifacial PV system, (5) fixed floating bifacial PV system with reflector, (6) horizontal-axis tracking floating monofacial PV system (0° tilt), (7) horizontal-axis tracking floating monofacial PV system (15° tilt), (8) horizontal-axis tracking floating bifacial PV system (0° tilt) with reflector, and (9) horizontal-axis tracking floating bifacial PV system (15° tilt) [Colour figure can be viewed at wileyonlinelibrary.com]

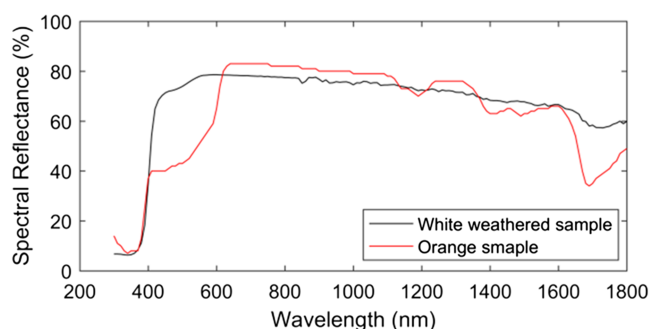


FIGURE 13 Measured spectral reflectance of the orange material (used in the pilot system) and a white weathered material (as a reference for comparison). The average reflectance (300–1800 nm) for the orange and white samples are 63.28% and 67.34%, respectively. Considering AM 1.5 spectrum, the broadband albedo (300–1800 nm) for the orange and white samples are 62.22% and 70.66% while the effective albedo (300–1200 nm, considering the response of mono-cSi) are calculated as 68.49% and 73.96%, respectively [Colour figure can be viewed at wileyonlinelibrary.com]

Moreover, this research practically considers reflectors and tracking systems to give a broader understanding about the performance of

various land-based and FPV systems. The monitoring of the nine pilot systems introduced in Section 3.3 is still an ongoing process. Several interesting points were recorded, observed, and examined that are discussed in Sections 4.1 to 4.6.

4.1 | Drifting pontoon

Less than 1 month after the installation, the modules on the fourth panel of the retractable system started to drift off and caused a drop in the electrical yield (maximum 50%) produced by that panel. This effect was noticed both via the camera at the site and by the recorded kWh by the optimizers. This issue started on the second week of October, detected in 2 weeks, and resolved in the second week of November (lasted for ~5 weeks).

4.2 | Storm events

The pilot systems experienced two storm events on February 9 and 16, 2020, storms Ciara and Dennis,^{61,62} with average wind

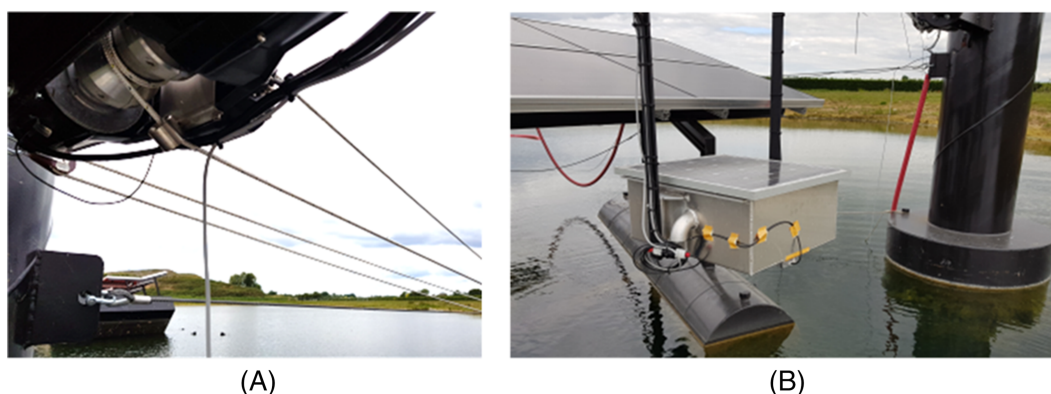


FIGURE 14 Components for the retracting system: (A) winch motor and cables, (B) photovoltaic + battery unit to power up the winch system [Colour figure can be viewed at wileyonlinelibrary.com]

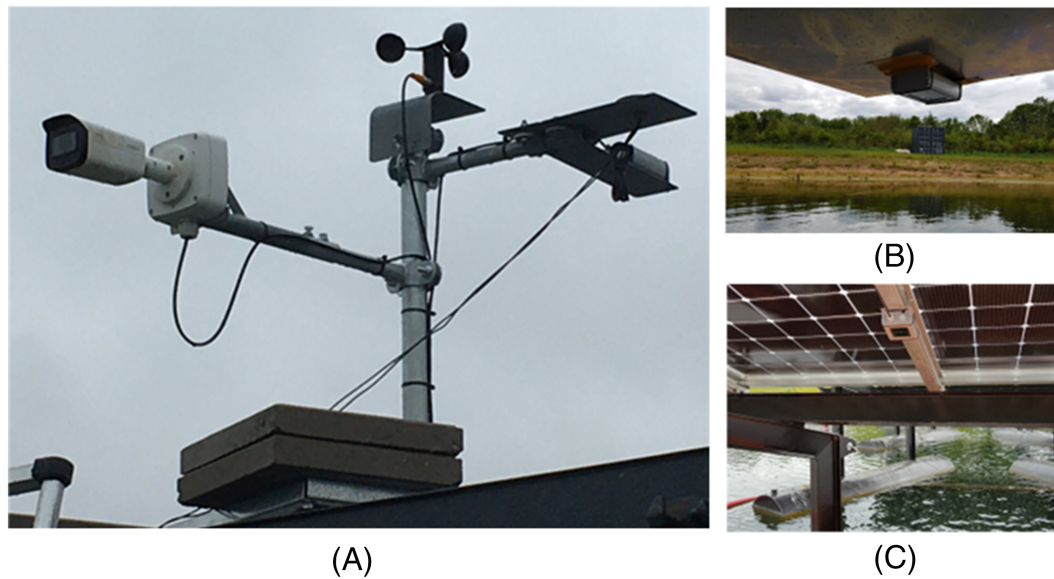
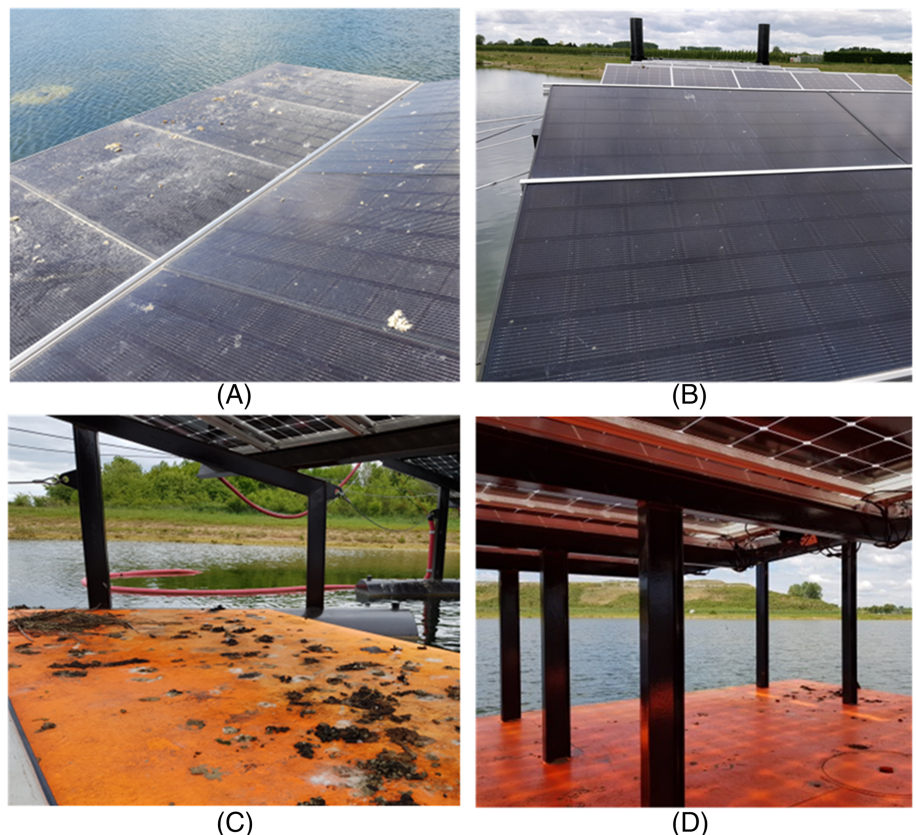


FIGURE 15 Sensors: (A) mete-unit consists a camera for occasional remote visual checks, anemometer to measured wind speed, temperature sensor to record ambient temperature, and a working-class reference cell to measured global horizontal irradiance, (B) a working class reference cell installed upside down to measure the sunlight reflected from the water, and (C) a working class installed at the rear side of a bifacial PV module (on the fourth panel of the retractable system) to measure the rear side irradiance [Colour figure can be viewed at wileyonlinelibrary.com]

speed of 50 km/h recorded at the pond (maximum wind gusts, measured at two of the closest meteo stations was ~ 90 – 97 km/h for both storm events). The systems did not damage and functioned normally during and after the storms with no yield

interruption. It is worth noting that during the same period, 1.5% of the Lingewaard FPV park (molded plastic-based pure floats) located at 10 km away from our pilot system was damaged by these storm events.⁴⁴

FIGURE 16 Birds influence on the floating pilot systems. (A) Horizontal pilot photovoltaic (PV) system no. 6 is considerably covered by birds droppings, whereas the tilted system on the same floater is much cleaner. (B) The tilted PV modules on the retractable floaters are barely influenced by birds. (C) Reflectors of the retractable systems that are placed horizontally and near the water level are easily accessible for the birds and, therefore, heavily fouled. On the left side of the image, a bird nest is also visible. (D) The reflectors on the floating island are much cleaner than the ones on the retractable system because the island reflector regularly tumbles and is more distant from the water level [Colour figure can be viewed at wileyonlinelibrary.com]



4.3 | Visual inspection

In May 2020, after almost 8 months of operation, a series of visual and thermal checks were done on the pilot systems. Visual checks were performed using the NREL guidelines for visual inspection.⁶³

(1) Slight azimuth misalignment was observed between the land-based pilot systems. It could be because of the storm event and/or inaccurate installation. Also, tilts of the land-based system deviated from the design (7° and 12.7° instead of 15°). However, the tilt and orientation of the FPV concepts were correct.

(2) Bird droppings were observed at several spots on the FPV modules. The influence of the bird presence was more intense for the surfaces that were closer to the water and less tilted. Remarkably, the reflectors of the retractable system (pilot system no. 5) and the horizontal monofacial PV modules on the tumbler floating island (pilot system no. 6) were heavily covered by bird droppings and even a bird nest (see Figure 16). It is worth noting that the other pilot systems were slightly soiled with no heavy shading.

A few passive actions can be done to reduce the birds' presence effects such as increasing the distance of the reflectors from the water level and placing them slightly tilted in the retractable system and keeping the floating island tumbled during the night time. However, this observation suggests more active bird control techniques (such as laser-based bird control⁶⁴) for inland FPV concepts.

(3) Vicinity to water: It was observed that when the floating island tumbles with high degrees, the monofacial modules on the (pilot systems nos. 6 and 7) almost touch the water surface. In the long term, this might boost the possibility for PID effect. However, this cannot be confirmed as long as electroluminescence or separate I-V measurements are done on the modules. This is out of the scope of the current study and is planned to be done after the full monitoring period.

4.4 | Thermal inspection

The thermal inspection was performed on the nine pilot systems on May 15, 2020, using a *Fluke Ti32* thermal imager. Several points were observed that are mentioned here.

The 1-day thermal inspection does not bring conclusive remarks about the temperature of the floating and land-based PV system. However, it is postulated that there should not be an overall significant temperature difference between the floating and land-based PV systems when they are placed close to each other, as long as they use the same PV technology. The reason is that the main cooling mechanism in PV systems is convective cooling mainly driven by the wind flow,⁶⁵ and both systems experience similar wind speeds. Moreover, due to the fact that the FPV modules are more exposed to the bird droppings, which cause shading⁶⁶ and hotspot,⁶⁷ in general, FPV modules compared with close-located land-based PV systems can even experience higher temperature spatial variance. Figure 17A,B shows the thermal images of the monofacial PV modules on the floating island and the land. As it can be seen, heavily fouled PV modules on the floating island experience higher spatial temperatures variance.

Another interesting aspect is the temperature difference between the front and rear sides of the floating bifacial PV modules. Figure 17C,D shows the thermal images of the front and rear sides of one module on the pilot system no. 9. Although the front side is experiencing a minor hotspot, the rear side has slightly (1.2°C) higher average temperature with more temperature nonuniformity.

4.5 | Irradiance monitoring

The irradiance sensors were used to monitor the real-time water albedo and the irradiance reflected on the rear side of the floating bifacial modules (to evaluate the contribution of the reflectors). The sensors installed and started to operate in May 2020. Results of the irradiance monitoring from May 23, 2020, to May 29, 2020, are shown in Figure 18A. For this duration, the daily average water albedo is about 11.6% with rises in the mornings and evenings because of the high angular dependency (low Lambertian behavior) caused by the low altitude of the sun. Also, it is interesting to observe that the water albedo increases during a cloudy day (May 24) with respect to a clear day (May 28) for about 4% absolute.

On daily average, the reflected irradiance on the rear side has a share of 23.4%. This ratio slightly decreases during the cloudy day with respect to a sunny day as a result of two opposite effects: the diffuse light in cloudy days increases the albedo of contributing surfaces (by casting less shadow on the ground²³), but on the other hand, the sunlight spectrum is less favorable for the orange-colored reflector (a cloudy day spectrum has more share in the high-frequency region⁶⁹).

In the mornings and evenings, PV systems receive low amount of sunlight; thus, the contribution of high morning and evening reflections in yield is very low; therefore, irradiance weighted albedo is a better parameter (than the average daily albedo), which was suggested by the literature.⁵⁹ Figure 18B shows the measured irradiance weighted albedo of the water and calculated irradiance weighted albedo of the orange reflector over a period of 4 months. Knowing the fact that the sensor at the rear side of bifacial PV panel sees both water and reflector, we used view factors^{23,70} (assuming Lambertian behavior) to obtain the irradiance weighted albedo of the reflector: *Reflected light ratio on the rear side* = $\alpha_{\text{reflector}} \times VF_{\text{reflector}} + \alpha_{\text{water}} \times VF_{\text{water}}$, where α is the albedo (no unit) and the VF is the view factor (no unit). View factors from the rear side of the bifacial PV panel to the reflector and water were calculated as $VF_{\text{reflector}} = 0.3313$ and $VF_{\text{water}} = 0.6687$, which show that for the retractable systems, the rear side of the bifacial modules see two thirds the water and one third the reflector. Now we can compare the effective albedo of the reflector before and after the heavy biofouling, which shows a drop from 68.49% to 24.21%, almost three times smaller.

4.6 | Electrical yield comparison

The specific DC yield (Wh/Wp) of the nine pilot systems were monitored 1 year, October 2019 until September 2020. The overall

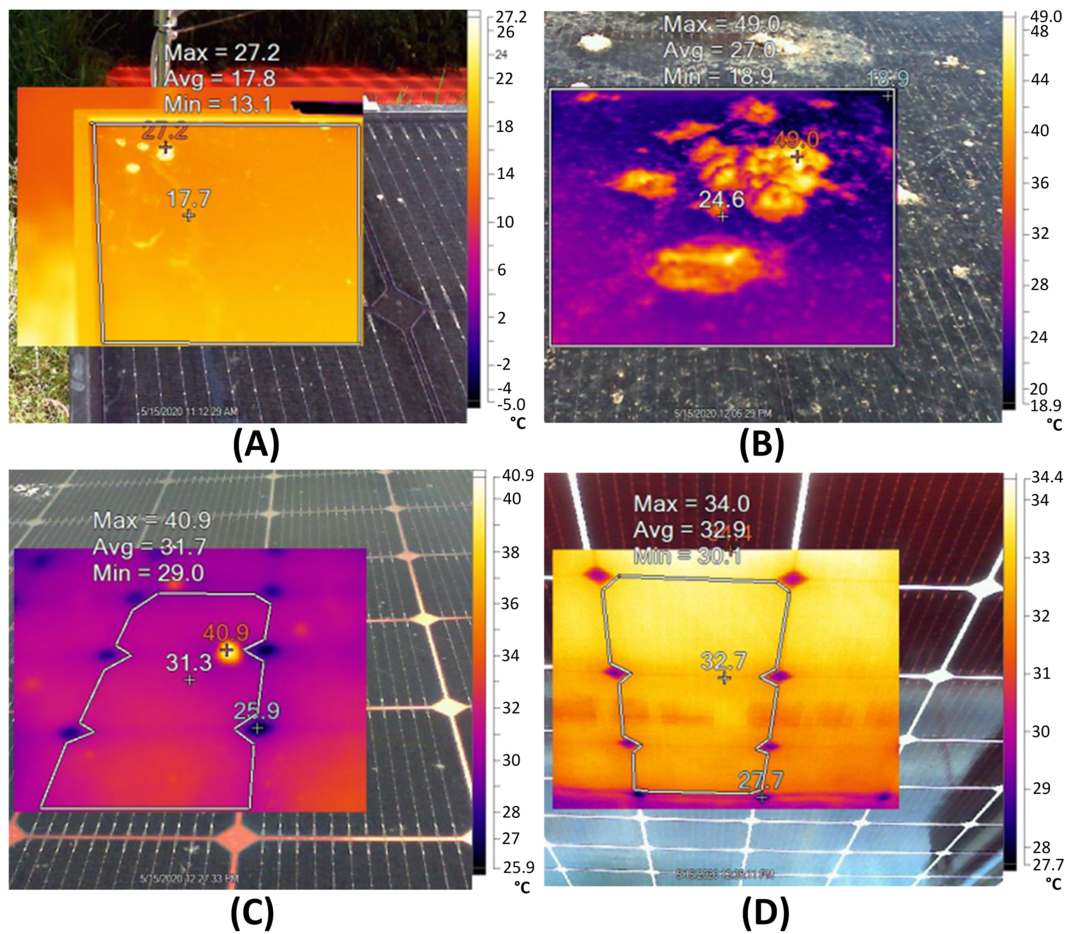


FIGURE 17 Thermophotography of the installed floating and land-based photovoltaic (PV) modules: (A) land-based monofacial PV module, (B) monofacial PV module on the floating island, (C) front side of one bifacial PV module on the floating island, and (D) rear side of the same bifacial PV module on the floating island. The min, max, and average temperature values for the area surrounded by the polygons are shown on the images. The temperature spatial variance, which is a key indicator of possible defects in thermal image-based diagnostics,⁶⁸ for (A) to (D) are 7.38, 26.72, 1.19, and 0.97°C.² Fluke Ti32 with coupled with SmartView software package was used to capture and analyze the thermal images. The average GHI and ambient temperature during these measurements were, respectively, 768 W/m² and 9.5°C [Colour figure can be viewed at wileyonlinelibrary.com]

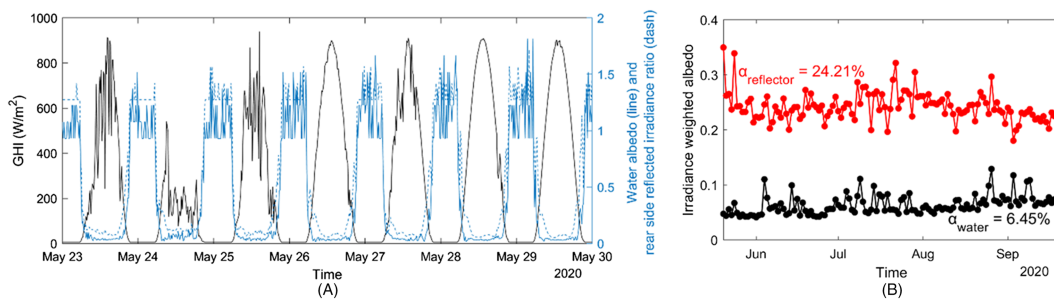


FIGURE 18 (A) Global horizontal irradiance, the albedo of the water, and the ratio of the reflected light on the rear side of the bifacial photovoltaic (PV) module, for one week in May 2020. The average daily water albedo and the rear side irradiance ratio of the floating bifacial PV module equipped with an orange-color reflector are 11.6% and 23.4%, respectively. For clear and cloudy days of May 28 and May 24, the water albedo is, respectively, 10.6% and 14.6%, whereas the rear side irradiance ratio is, respectively, 24.3% and 22.9%. The values were obtained excluding the nighttime recordings. (B) Irradiance weighted albedo of water and reflector from May 20, 2020, to September 20, 2020. Mean values are depicted on the graph, which shows bio-fouling severely reduces the effective albedo of the reflector from 68.49% to 24.21% [Colour figure can be viewed at wileyonlinelibrary.com]

performance of the systems is shown in Figure 19 and further broken down into the monthly comparison in Figure 20. The comparison shows that the tracking bifacial modules with reflector (system no. 9)

outperform all the other systems by yielding ~17.3% more than the reference land-based monofacial modules (system no. 1, as a reference). In a month with more clear sky days (May 2020), this value

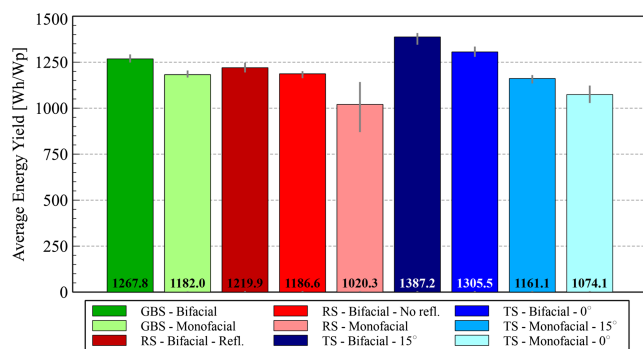


FIGURE 19 Comparison of the overall specific DC yields of the pilot photovoltaic systems after 1 year of monitoring (October 2019 to September 2020). The green bars represent the ground-based system, the red bars the retractable system, and the blue bars the tracker system. The gray error bars depict the range of the minimum and the maximum energy yield of each module in the respective system. GBS: ground-based system, TS: tracking system, RS: retractable system, refl: reflector [Colour figure can be viewed at wileyonlinelibrary.com]

reaches up to ~29%. The bifacial modules on the retractable floater (systems no. 4 and no. 5), however, produce less than the land-based bifacial modules (systems no. 2), proving the effect of low water albedo and severe influence of the birds' presence on the reflectors of the retractable system. It is worth noting that the pilot systems no. 3 and no. 6 are, respectively, experiencing less favorable sunlight and temperature. System no. 5 is regularly shaded over a few hours a day by the front anchoring poles (caused ~10% drop in energy production), and system no. 6 can barely benefit from backside cooling as it is attached to the surface of the floating island. To avoid shading, in the future designs, the front poles will be shorter, and when upscaling, there will be mutual poles between the retractable systems, which reduces the number of poles and the chance for shading.

4.7 | Ecological impacts

Knowledge on the ecological impacts of FPV systems is limited. Currently, most scientific work has focused on the technological advancements, rather than the impacts to the environment.^{71,72} When environmental impacts are assessed, the focus is either on temperature^{73,74} or fish production,⁷⁵ rather than impacts on lake ecological functioning. Studies addressing the potential impacts of FPV on ecosystem are, to-date, theoretical in their scope.⁷⁶ In order to understand the effects of the installed pilot FPV systems on the ecosystem, a large number of measurements were made under and in the vicinity of the floating pilot setup (see Figure 21A for ecological tests spots in the pond):

1. Water quality (August to September 2019)
2. Temperature logger (September 2019 to July 2020)
3. Camera trap, to register movements of animals (December 2019)
4. Aquatic plants biomass (September 2019)

5. Oxygen logger (September–December 2019 and March–July 2020)

The results of each ecological measurement is discussed in the following five paragraphs.

For water quality assessment, total nitrogen (TN), total phosphorus (TP), chlorophyll-a, a measure of total phyto-plankton abundance (Chl-a), and cyanobacterial chlorophyll, a measure of potentially toxic cyanobacterial abundance (cyano-Chl), were measured by weekly sampling. This traditional water quality monitoring showed no significant differences in relevant water quality parameters.

High frequency monitoring of water temperature was carried out using continuous loggers (HOBO MX2202; 5 min logging interval) positioned at the top and bottom part of the water column (at test spots 1, 4, and 5 in Figure 21A). Temperature did not differ greatly under the FPV systems compared with the control site (spot 5) throughout the winter period (<0.1°C). Spring temperatures were around 0.2°C on average lower under both FPV setups. Summer water temperatures under the FPV systems were also decreased by an average of 0.8°C, which may cause less local evaporation⁷⁴ and have a local effect on the proliferation of phytoplankton.⁷⁷

Camara traps placed on and around the FPV structures revealed that the FPV systems were repeatedly visited by (water) birds (see Figure 21B). Although birds do visit the FPV systems, the number of birds and the frequency of their visits seemed to be low. However, even these low number of visits had consequences for the performance of the PV systems in short term (see Sections 4.3 to 4.5).

Submerged aquatic plants are a vital part of a healthy shallow lake ecosystem, hampering algal blooms, providing habitat for other organisms, and capturing suspended particles.⁷⁸ Hence, the impact of the pilot setup on this biotic group is of great importance to understand. A significantly higher biomass of aquatic plants was observed in between the FPV systems than under either of the two setups (see Figure 21C). Whereas biomass was comparable to spot 5 (Figure 21C), the species of plants growing here were different (resp. *Elodea nutallii* and *Stuckenia pectinate*). This shows that, although plant growth was possible under the PV systems, it was reduced by a factor three. These results need to be seen in the light of plant life cycles. The PV setups were installed after the plants had already established, that is, after their most critical life stages (germination and sprouting). Hence, although aquatic plant growth in reduced form is possible under the PV setups, long-term persistence may still be hampered.

Low oxygen concentrations can lead to harmful effects for biota, with concentrations <5 mg/L being harmful to fish populations and <1 mg/L leading to large scale fish kills.^{79,80} Moreover, sediment anoxia (lack of oxygen) can lead to increased nutrient loading by breaking biogeochemical bonds between phosphorus and iron. The effectiveness of these iron-phosphorus bounds is already compromised at levels of $O_2 < 6$ mg/L.⁸¹ Also, methane (a powerful greenhouse gas) is produced under such anoxic conditions, leading to increased greenhouse gas emissions from lakes.⁸² Two oxygen loggers were placed on the sediment at test spots 1 and 5 to record oxygen dynamics. Overall, anoxic

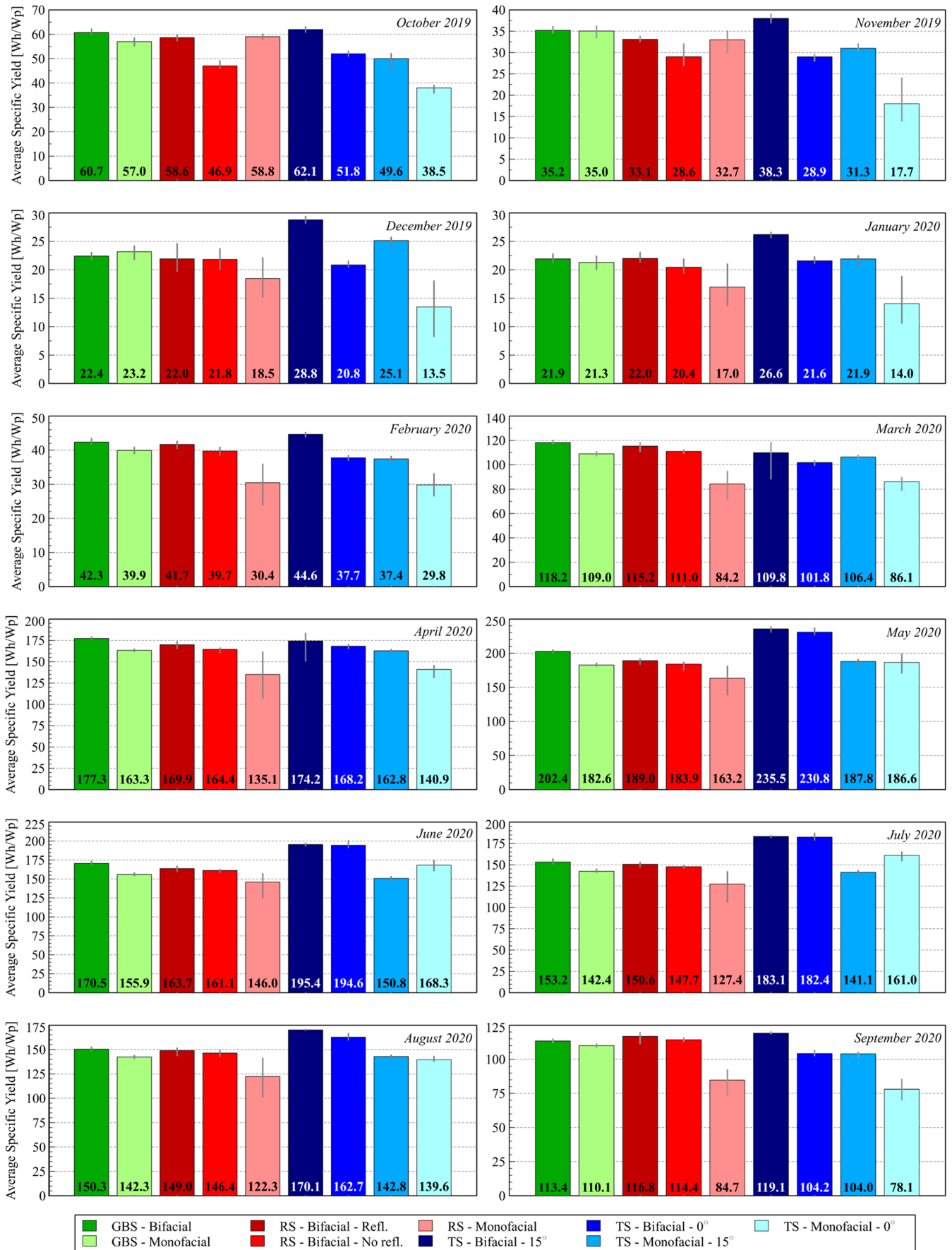


FIGURE 20 Monthly breakdown of the specific yield for the monitored pilot systems. The green bars represent the ground-based system, the red bars the retractable system, and the blue bars the tracker system. The gray error bars depict the range of the minimum and the maximum energy yield of each module in the respective system. In 1 year, the pilot systems on the floating island have produced 7.26 MWh in total. This means sun-tracking consumes 0.45% of the production (see pumps consumption calculation in Section 3.4). GBS: ground-based system, TS: tracking system, RS: retractable system, ref: reflector [Colour figure can be viewed at [wileyonlinelibrary.com](#)]

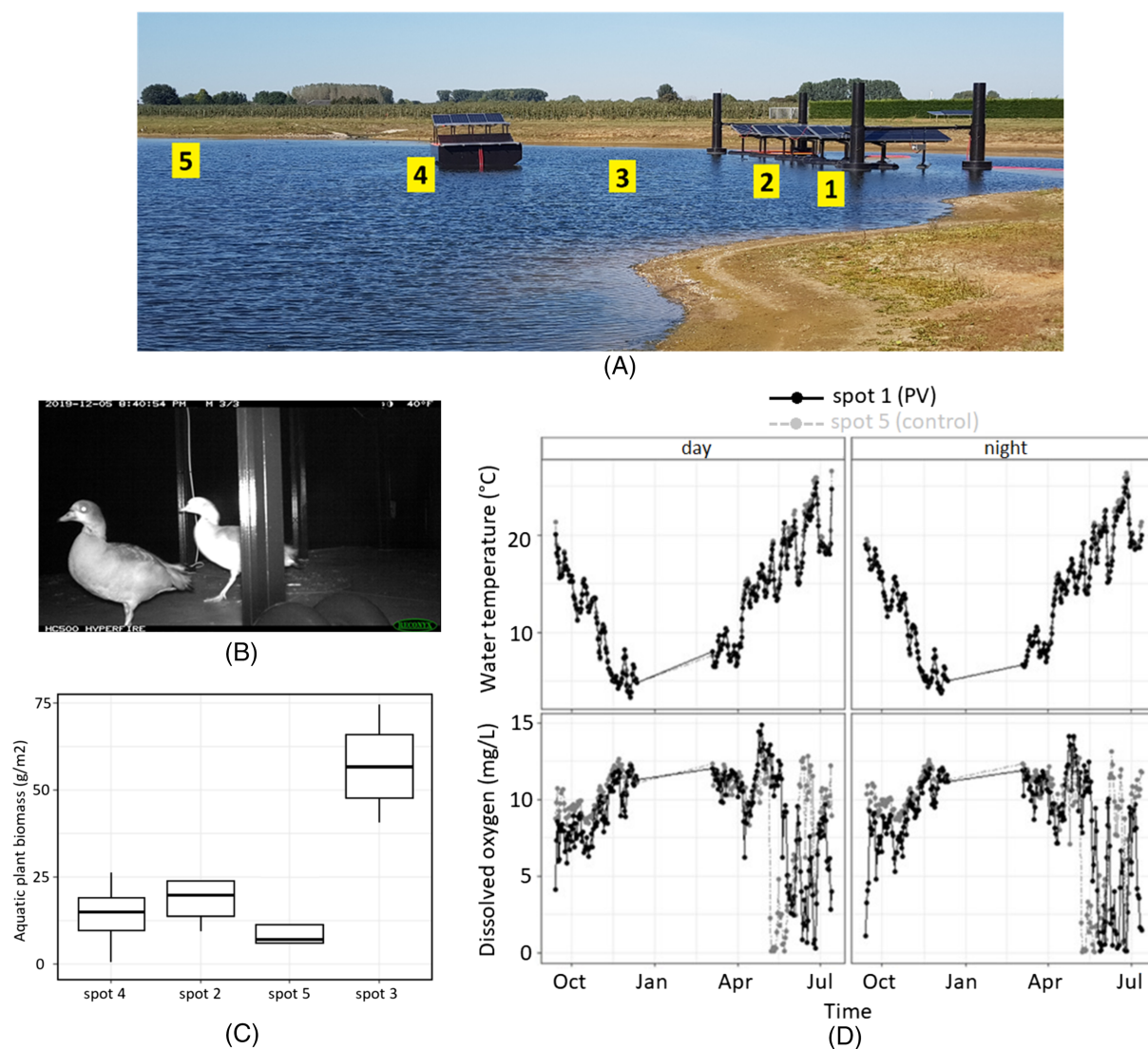


FIGURE 21 Results of ecological monitoring. (A) Spots in the pond where measurements were taken. Spots 1 and 2 are below the retractable system, respectively, under the first and third rows of the panels; thus, one has reflector, the other has not. Spot 3 is between the retractable and floating island. Spot 4 is under the floating island. Spot 5 (control site) is located out of the sphere of influence of the FPV structures. (B) Camera traps captured a pair of Nile geese visiting the floating island structure. Within 2 weeks, the pair visited the floating island on four different occasions. (C) Plant biomass in g/m² for the different experimental spots. For each spot, four subplots were harvested. Further, harvested material was dried for 96 h at 60°C and then weighted. The control site (spot 5), also showed a lower plant biomass than the site between FPV structures (spot 3). However, the species growing at the control site was identified as *Stuckenia pectinata* whereas aquatic plant species found both between and under the FPV structures were identified as waterweed (*Elodea nuttallii*). While both plant types are fast growers, *Elodea* is known to be a very sturdy plant that does well even under disturbed conditions. (D) Temperature at the bottom and dissolved oxygen in mg/L under the retractable PV system (spot 1) and at a control site (spot 5) averaged for both day and night [Colour figure can be viewed at [wileyonlinelibrary.com](#)]

conditions (more than three consecutive measurements of <1 mg/L anoxia) were found to occur 68 days or nights for the control site and 65 times under the FPV system. Hence, we can conclude that extreme anoxia was not found to be more likely underneath the FPV systems in

the study location. Hypoxic conditions (defined as consecutive periods with more than three measurements of <6 mg/L O₂) were found to occur much more frequently underneath the PV setups compared with the open water site (spot 5) (resp. 157 times vs. 87) (see Figure 21D).

Such an impact of FPV on oxygen concentrations in the water column can be attributed either to increased consumption of oxygen or decreased production. Plant growth was diminished underneath the panels, which suggests that primary production through photosynthesis will be lower under the PV setup. However, increase in microbial processes consuming oxygen cannot be disregarded, as changes in wind action around the panels may impact sediment formation processes. Regardless of the cause of the increased hypoxia underneath the PV setups, its impact to the ecosystem (e.g., internal loading, impact on fish, and greenhouse gas emissions) can be far reaching. Considering the small scale of the pilot setup and its open nature, these results show that increased attention for the environmental impacts of FPV systems is necessary.

5 | CONCLUSION

This paper introduced two novel FPV concepts for inland water areas: the retractable and the tumbler island. The introduced concepts can accommodate bifacial PV modules equipped with reflectors and horizontal sun tracking. They also do not disturb mowing activities and can be moved around to enable light penetration into the water. The location survey, modeling, realization, and the results of 1-year monitoring were reported. Through the study, several facts about floating bifacial PV were revealed that oppose the traditional claims. A summary of outcomes is mentioned below.

1. Despite the immediate expectation, inland water areas have low effective albedo (6.5%) which makes water less favorable for bifacial PV installation. Therefore, including reflectors is highly recommended.
2. Frame soaking of the FPV modules has a very minor influence (<0.2%) on the performance and, therefore, does not bring added values.
3. Horizontal sun tracking is possible for FPV structures by adjusting the water content within the floater compartments by the pumps. This approach consumes low amount of tracking energy (<0.5% of the produced energy).
4. The birds' presence on the floaters show its effect in the short term (e.g., bio-fouling reduced the effective albedo of the reflectors from 68% to 24% in 8 months). The surfaces that directly (PV) and indirectly (reflector) play a role in the FPV irradiance capturing should be kept tilted and at a higher level than that of the water. This reduces the birds' presence effects. Active bird control techniques are also recommended.
5. FPV system experience higher bio-fouling rate and will suffer more from temperature spatial variance compared with land-based PV systems located close by. This will boost the aging procedure.
6. Quantitative yield monitoring and analysis revealed that only bifacial PV with a reflector and limited angle horizontal tracking can outperform the conventional land-based systems considerably (by 17.3%).
7. Results showed no significant differences in relevant water quality parameters (TN, TP, Chl-a, and cyano-Chl) and water temperature (<0.8°C) when FPV systems are installed. However, already established aquatic plants accumulate three times less biomass under the FPV systems.
8. Under the FPV systems, periods of hypoxia (<6 mg/L O₂) are much more frequent, and anoxia was not found to occur more frequently.

The reported findings and the lessons learned will help the FPV community to identify knowledge gaps, tackle challenges, and improve designs to achieve technological readiness of such setups for the water sector.

ACKNOWLEDGEMENTS

The work was supported by the Renewable Energy subsidy from The Netherlands Enterprise Agency (RVO) via the project: INNOZOWA with Grant No. TEHE116369. The subsidy aims at making the production of renewable energy more affordable through innovative technologies, including PV solar technology. The authors would like to thank Nynke Hermelink (RVO), Johan Bakker (Waterschap Rivierenland), Peter van der Linde (Hakkers BV), Furkan Fatih Sönmez (TU Delft), and Andres Calcabrini (TU Delft), respectively, for organizational suggestions, practical discussion, suggestions for mechanical design, help in measurements, and comments on simulations. The authors would also like to thank Dianneke van Wijk (WUR, NIOO-KNAW), Lilith Kramer (NIOO-KNAW), Dennis Waasdorp (NIOO-KNAW), and Erik Vennings (AQUON) for assistance with ecological data collection in the field.

Data Availability Statement

The data that support the findings of this paper are available from the corresponding author upon reasonable request.

ORCID

Hesan Ziar  <https://orcid.org/0000-0002-9913-2315>

Olindo Isabella  <https://orcid.org/0000-0001-7673-0163>

REFERENCES

1. Luque A, Cuevas A, Ruiz J. *Double-Sided N+–P–N+ Solar Cell for Bifacial Conc Solar Cells*. 1980;2(2):151-166.
2. Global Bifacial Module Market Report 2019. 2020, Wood Mackenzie Power & Renewables.
3. Equipment, V.P., International Technology Roadmap for Photovoltaic (ITRPV) 2019 Results. 2020, March.
4. Abel GJ, Barakat B, Samir KC, Lutz W. Meeting the sustainable development goals leads to lower world population growth. *Proc Natl Acad Sci*. 2016;113(50):14294-14299.
5. Dutch water facts. 30-05- 2020]; Available from: <https://www.holland.com/global/tourism/information/general/dutch-water-facts>
6. Taboada M et al. Solar water heating system and photovoltaic floating cover to reduce evaporation: experimental results and modeling. *Renew Energy*. 2017;105:601-615.
7. Romijn Maarten, Head of R&D, HydroPV, personal communication, March 24, 2020.

8. Golroodbari SZ. and van Sark W. Simulation of performance differences between offshore and land-based photovoltaic systems. *Progress in Photovoltaics: Research and Applications*, 2020.
9. Sharma P, Muni B, Sen D. Design parameters of 10 KW floating solar power plant. *Proc Inter Adv Res J Sci, Engin Tech (IARJSET)*, National Conf on Rene Energy Envir (NCREE-2015), Ghaziabad, India. 2015;2: 85-89.
10. Ferrer-Gisbert C et al. A new photovoltaic floating cover system for water reservoirs. *Renew Energy*. 2013;60:63-70.
11. Sahu A, Yadav N, Sudhakar K. Floating photovoltaic power plant: a review. *Renew Sustain Energy Rev*. 2016;66:815-824.
12. Maisch, M., *WoodMac: Bifacial module capacity will exceed 21 GW by 2024*, in *PV Magazine*. 2019.
13. <https://www.waterschaprivierenland.nl/>
14. <https://www.hakkers.com/>
15. <https://www.blue21.nl/>
16. Mondol JD, Yohanis YG, Norton B. Solar radiation modelling for the simulation of photovoltaic systems. *Renew Energy*. 2008;33(5):1109-1120.
17. Oke TR. The energetic basis of the urban heat island. *Q J Roy Meteorol Soc*. 1982;108(455):1-24.
18. Sönmez FF et al. Fast and accurate ray-casting-based view factor estimation method for complex geometries. *Solar Ene Mate Solar Cells*. 2019;200:1-9, 109934.
19. <https://meteonorm.com/en/product/horicator>
20. Meteonorm 7.3.4. Available from: <https://meteonorm.com/en/download>
21. Steyn D. The calculation of view factors from fisheye-lens photographs: Research note. 1980.
22. Keijzer M. A multi-surface reflected irradiance model for pyranometer corrections and PV yield calculations in complex urban geometries. 2019, Delft University of Technology
23. Ziar H et al. A comprehensive albedo model for solar energy applications: geometric spectral albedo. *Appl Energy*. 2019;255:1-16, 113867.
24. Brennan M et al. Effects of spectral albedo on solar photovoltaic devices. *Solar Ene Mate Solar Cells*. 2014;124:111-116.
25. Flyer: Reference cells, Spectral response of different reference cells, I. Fraunhofer, Editor.
26. Guerrero-Lemus R et al. Bifacial solar photovoltaics—a technology review. *Renew Sustain Energy Rev*. 2016;60:1533-1549.
27. Liang TS et al. A review of crystalline silicon bifacial photovoltaic performance characterisation and simulation. *Energ Environ Sci*. 2019;12(1):116-148.
28. Khatib T, Mohamed A, Sopian K. A review of solar energy modeling techniques. *Renew Sustain Energy Rev*. 2012;16(5):2864-2869.
29. Standard ASTM. G173-03-Standard tables for reference solar spectral irradiances: direct normal and hemispherical on 37 tilted surface. *Ann. Book of ASTM Standards* 2003. 2012;14:1-20.
30. Carolus J et al. Physics of potential-induced degradation in bifacial p-PERC solar cells. *Solar Ene Mate Solar Cells*. 2019;200:1-6, 109950.
31. KNMI - Koninklijk Nederlands Meteorologisch Instituut. Available from: <https://www.knmi.nl/home>
32. Watson DF, Philip G. A refinement of inverse distance weighted interpolation. *Geobiology*. 1985;2(4):315-327.
33. Ridley B, Boland J, Lauret P. Modelling of diffuse solar fraction with multiple predictors. *Renew Energy*. 2010;35(2):478-483.
34. Mishra S. *Selection Map for PV Module Installation Based on Shading Tolerability and Temperature Coefficient*. Delft University of Technology; 2018.
35. de Vries TN et al. A quick-scan method to assess photovoltaic rooftop potential based on aerial imagery and LiDAR. *Solar Energy*. 2020;209: 96-107.
36. Santbergen R et al. Annual energy yield simulation toolbox and its application to floating bifacial photovoltaic modules with reflectors. In: *ELECTRIMACS 2019*. Salerno, Italy, 21st-23rd May 2019; 2019.
37. Cazzaniga R et al. Floating photovoltaic plants: performance analysis and design solutions. *Renew Sustain Energy Rev*. 2018;81:1730-1741.
38. Peter N et al. 3D finite element method modelling and simulation of the temperature of crystalline photovoltaic module. *Intern Research in Engin and Tech*. 2015;4(9):378-384.
39. Harvey R et al. The influence of air temperature on water temperature and the concentration of dissolved oxygen in Newfoundland Rivers. *Can Water Res J*. 2011;36(2):171-192.
40. Lausch D et al. Potential-induced degradation (PID): introduction of a novel test approach and explanation of increased depletion region recombination. *IEEE J Photovo*. 2014;4(3):834-840.
41. Trapani K, Redón Santafé M. A review of floating photovoltaic installations: 2007–2013. *Progress in Photov: Res App*. 2015;23(4):524-532.
42. Schmaelzle PH et al. Deployment techniques of a floating photovoltaic power generation system. 2017, Google Patents.
43. Water WSM. Floating Solar Market Report. World Bank Group and SERIS, Singapore, 2018.
44. Another damage to floating solar park Lingewaard, in *Solar Magazine*. 2020.
45. Bellini, E., Japan's largest floating PV plant catches fire after Typhoon Faxai impact, in *PV Magazine*. 2019.
46. HYDRELIO® technology: <https://www.ciel-et-terre.net/hydrilio-floating-solar-technology/hydrilio-products/>. 2020.
47. Floating solar: Europe's largest power plant is French, <https://www.planet.veolia.com/en/floating-solar-power-plant-piolenc-france>. 2019.
48. Cazzaniga, R., *Floating PV Plants*. Chapter 4: Floating PV Structures. 2020: Academic Press.
49. Floating in the Alps, *PV magazine*, November 2019. <https://www.pv-magazine.com/2019/11/18/floating-in-the-alps/>
50. Tina G, Rosa-Clot M, Rosa-Clot P. Electrical behavior and optimization of panels and reflector of a photovoltaic floating plant. *Proc 26th European Photov Solar Energy Conf Exhib (EU PVSEC'11)*. 2011;1-5.
51. Clot MR, Clot PR, and Carrara S. Apparatus and method for generating electricity using photovoltaic panels. 2011, Google Patents
52. Fraas, L., et al., Solar PV carousel trackers for building flat rooftops: Three case studies 2010.
53. Correia N et al. Solar panel tracking system. 2019, Google Patents.
54. Correia N et al. Rotating floating platform. 2020, Google Patents.
55. Folkerts W et al. Roadmap PV Systemen en Toepassingen. 2017.
56. UNIQUE RESEARCH FLOATING SOLAR PANELS HAS STARTED. <https://www.tno.nl/nl/aandachtsgebieden/energietransitie/roadmaps/naar-een-overvloed-aan-zonnestroom/zonne-energie-slim-integreren-in-onze-leefomgeving/uniek-onderzoek-drijvende-zonnepanelen/>. 2020.
57. Yadav N, Gupta M, Sudhakar K. Energy assessment of floating photovoltaic system. In: *2016 International Conference on Electrical Power and Energy Systems (ICEPES)*. IEEE; 2016.
58. Choi Y-K, Lee N-H, Kim K-J. Empirical research on the efficiency of floating PV systems compared with overland PV systems. *Proc, The 3rd Inter Conf Circuits, Control, Comm, Electr, Elect, Energy, Sys, Signal and Simu*. 2013;681-685.
59. Liu H et al. Field experience and performance analysis of floating PV technologies in the tropics. *Progress in Photovoltaics: Research and Applications*. 2018;26(12):957-967.
60. Choi Y-K. A study on power generation analysis of floating PV system considering environmental impact. *Intern J Software Engin App*. 2014; 8(1):75-84.
61. https://en.wikipedia.org/wiki/Storm_Ciara
62. https://en.wikipedia.org/wiki/Storm_Dennis

63. Packard CE, Wohlgemuth JH, Kurtz SR. *Development of a Visual Inspection Data Collection Tool for Evaluation of Fielded PV Module Condition*. CO (United States): National Renewable Energy Lab. (NREL), Golden; 2012.
64. <https://www.birdcontrolgroup.com/>
65. Jones A, Underwood C. A thermal model for photovoltaic systems. *Solar Energy*. 2001;70(4):349-359.
66. Ziar H et al. Quantification of shading tolerability for photovoltaic modules. *IEEE J Photovo*. 2017;7(5):1390-1399.
67. Ziar H et al. Bypass diode characteristic effect on the behavior of solar PV array at shadow condition. In: *2012 3rd Power Electronics and Drive Systems Technology (PEDSTC)*. IEEE; 2012.
68. Tsanakas J, Botsaris P. An infrared thermographic approach as a hot-spot detection tool for photovoltaic modules using image histogram and line profile analysis. *Intern J Cond Monit*. 2012;2(1):22-30.
69. Bird RE, Riordan C. Simple solar spectral model for direct and diffuse irradiance on horizontal and tilted planes at the earth's surface for cloudless atmospheres. *J Clim Appl Meteorol*. 1986;25(1):87-97.
70. Gross U et al. Shapefactor-equations for radiation heat transfer between plane rectangular surfaces of arbitrary position and size with parallel boundaries. *Lett in Heat Mass Trans*. 1981;8(3):219-227.
71. Ranjbaran P et al. A review on floating photovoltaic (FPV) power generation units. *Renewable and Susta Ener Rev*. 2019;110:332-347.
72. Sahu A et al. Floating photovo power plant: A review. *Renewable and Sustainable Energy Reviews*. 2016;66:815-824.
73. Zhang N et al. High-performance semitransparent polymer solar cells floating on water. *Rati Anal Power Gene, Water Evapor and Algal Growth*. 2020;77:1-11, 105111.
74. Ferrer-Gisbert C et al. A new photovoltaic floating cover system for water reservoirs. *Renewable Energy*. 2013;60:63-70.
75. Pringle AM et al. Aquavoltaics: synergies for dual use of water area for solar photovoltaic electricity generation and aquaculture. *Renew Sustain Energy Rev*. 2017;80:572-584.
76. Cagle AE et al. The land sparing, water surface use efficiency, and water surface transformation of floating photovoltaic solar energy installations. *Sustainability*. 2020;12(19-8154):11-22.
77. Velthuis M et al. Warming advances top-down control and reduces producer biomass in a freshwater plankton community. *Ecosphere*. 2017;8(1):1-16, e01651.
78. van Donk E, van de Bund WJJAb. Impact of submerged macrophytes including charophytes on phyto-and zooplankton communities: allelopathy versus other mechanisms. *Aquatic Botany*. 2002;72(3-4): 261-274.
79. Nürnberg GKJ. Quantification of oxygen depletion in lakes and reservoirs with the hypoxic factor. *Lake and Reservoir Management*. 2002; 18(4):299-306.
80. Rao YR et al. On hypoxia and fish kills along the north shore of Lake Erie. *J Great Lakes Res*. 2014;40(1):187-191.
81. Smolders A et al. Controlling phosphate release from phosphate-enriched sediments by adding various iron compounds. *Biogeochemistry*. 2001;54(2):219-228.
82. Sepulveda-Jauregui A et al. Eutrophication exacerbates the impact of climate warming on lake methane emission. *Sci Total Environ*. 2018; 636:411-419.

How to cite this article: Ziar H, Prudon B, Lin F-Y, et al. Innovative floating bifacial photovoltaic solutions for inland water areas. *Prog Photovolt Res Appl*. 2021;29:725-743. <https://doi.org/10.1002/pip.3367>